

Mechanical properties of Nafion™ electrolyte membranes under hydrated conditions

Sumit Kundu^a, Leonardo C. Simon^{a,*}, Michael Fowler^a, Stephen Grot^b

^a Department of Chemical Engineering, University of Waterloo, 200 University Avenue West, Waterloo, Ont., Canada N2L 3G1

^b Ion Power Inc., 720 Governor Lea Rd., New Castle, DE 19720, USA

Received 24 June 2004; received in revised form 27 January 2005; accepted 12 September 2005

Available online 21 October 2005

Abstract

Polymer electrolyte membrane fuel cells use a polymer membrane as the electrolyte to transport hydrogen ions from the anode to the cathode side. This paper reports a study of mechanical (stress–strain curves) and dynamic mechanical (temperature sweeps) properties of membranes made using Nafion™ under dry and hydrated conditions. Hydrating the membranes reduced the mechanical properties. Specifically there was significant change in the Young's modulus, yield strength, and transition temperatures of the different membranes tested. Presence of contaminant ions was studied through an ion exchange technique using selected ions (Na^+ , K^+ , Mg^{2+} , Cu^{2+} , Ni^{2+}). Ion exchange in hydrated samples increased the stiffness of the material as well as the yield strength in order of increasing ionic radius. Transition onset temperatures observed on the mechanical damping of hydrated membranes also increased with the addition of ions.

© 2005 Elsevier Ltd. All rights reserved.

Keywords: Nafion™; Mechanical testing; DMTA

1. Introduction

Fuel cells are electrochemical devices that react chemicals to produce electric power like a battery except that the reactants can be continuously supplied. Polymer electrolyte membrane fuel cells (PEMFCs) catalytically react hydrogen and oxygen to produce electricity and water. The main benefits of PEMFCs are that they can produce power without any harmful emissions from their use and at higher efficiencies than internal combustion engines. As such, PEMFCs are one of the leading clean energy technologies being considered for residential power generation needs as well as in transportation applications. However, there are still many barriers to market penetration of this technology, including a poor understanding of material degradation and durability issues [1].

The heart of the PEMFC is the polymer electrolyte which acts as a gas barrier between the anode and cathode as well as a hydrogen ion conductor. The most common commercially available membrane used today is Nafion™ produced by Dupont. Nafion™ is a perfluorosulfonic acid polymer membrane

consisting of a Teflon-like backbone with side chains ending with $-\text{SO}_3\text{H}$ groups, as shown in Fig. 1. The presence of three distinct phases [2] in Nafion™ has been confirmed by numerous studies including transmission electron microscopy analysis [3], small angle X-ray scattering [4], and atomic force microscopy [2]. The first region is a hydrophobic semicrystalline region primarily made up of the backbone chains. The backbone provides structural stability to the membrane and prevents it from dissolving in water [4]. The second region is a largely empty amorphous region that consists of side chains and some sulfonic acid groups. The final region consists of clusters of the hydrophilic sulfonic acid groups which are responsible for conducting protons across the membrane. Ion conduction can only occur at the desired rates when the membrane is hydrated with water. Therefore, a fuel cell typically operates with fully humidified anode and cathode gas streams. Water produced at the cathode also contributes to the hydration of the membrane. Poor ionic conduction through the membrane results in ohmic losses and consequently poor performance during fuel cell operation. Contamination of the membrane is possible during fuel cell operation. Contaminant ions such as Na^+ , K^+ , Mg^{2+} , Cu^{2+} , and Ni^{2+} can taint the membrane through ion exchange with the hydrogen ions. Sources of contamination include impure feed gasses, corrosion of components in the gas distribution system,

* Corresponding author. Tel.: +1 519 8884567x3301; fax: +1 519 7464979.
E-mail address: lsimon@uwaterloo.ca (L.C. Simon).

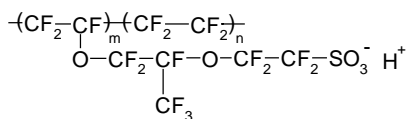


Fig. 1. Chemical structure of Nafion™ where $m=6-10$ and $n=1$.

fittings, or tubing, as well as ions in the water supply [5,6] that is needed to hydrate the reactant streams.

Understanding the mechanical properties of the membrane is essential to produce high quality membranes with good durability and long lifetimes [7] under typical fuel cell operating conditions. Previous work included mechanical testing reported by Kawano et al. [8] which showed that the mechanical properties of Nafion™ membranes were influenced by both hydration and metal ions. They found that Nafion™ soaked in water or different solutions of methanol or ethanol reduced the Young's Modulus compared to the membrane as received. This group also examined the effects of ions from the first group of the periodic table (alkali metals) and found that the Nafion™ membranes became stiffer with the addition of the metal ions. Specifically, the initial slopes increased following a salt order of Li^+ , Na^+ , K^+ , Cs^+ , and Rb^+ . The salt forms of the membranes were dried in a vacuum oven prior to testing. Yeo and Eisenberg [9] conducted studies into the dynamic mechanical properties of Nafion™. Using dynamic mechanical experiments they found 4 transitions in the Nafion™ membrane over a temperature range of $-150-250$ °C. The most relevant peak was the α peak at temperatures of 150 °C. This peak was assigned to the glass transition temperature of the ionic regions. The existence of transitions between 100 and 150 °C has been further corroborated by other groups using dynamic mechanical thermal analysis (DMTA) and differential scanning calorimetry (DSC) [10–13]. None of these studies had examined the material under fully hydrated conditions. In a fuel cell, the membrane may be exposed to liquid water through the cathode water production which may even lead to flooding as well as water condensation at the anode due to the drop in hydrogen pressure as a consequence of hydrogen consumption. Few studies examined Nafion™ in a fully hydrated state. Kyu and Eisenberg [14] measured the under-water and the undermethanol stress relaxation of Nafion™ and concluded that the glass transition was profoundly influenced by the presence of water and that methanol was also able to interact with non-ionic domains in the membrane. Uan-Zo-Li [10] studied the plasticization effect of water by performing dynamic mechanical testing using a three point bending

technique with the test fixture submerged in water and found a reduction in the dynamic moduli of the material.

This paper investigates mechanical properties of membrane electrolyte assemblies and Nafion™ membranes through isothermal stress–strain curves for determination of Young's modulus and yield strength and through temperature sweeps in the dynamic-mechanical thermal analysis for determination of storage and loss moduli and mechanical damping. The properties were measured under dry and fully hydrated conditions using a dynamic mechanical thermal analyzer in an inverted position with the sample immersed in water or salt solutions. The impact of contaminant ions on the mechanical properties of hydrated membranes was also examined.

2. Experimental

2.1. Materials

The membranes were provided by Ion Power Inc. and are summarized in Table 1. Two types of membranes were used in this study: (a) those that were composed solely of Nafion™; and (b) membrane electrolyte assemblies (MEA), called here catalyzed membranes, composed of Nafion™ membrane coated in 3 mg/cm^2 Pt/C catalyst layer in a Nafion substrate. Membrane 522B, a catalyzed membrane, served as the starting point for this study. Membranes Nafion™ 117 and Nafion™ 112 are pure solution cast Nafion™ membranes and were used for comparison in the hydrated mechanical tests. All other membranes were catalyzed membranes and used Nafion™ 112 as their core electrolyte. In the case of membrane 144A, samples of new and 'aged' membrane (i.e. the membrane had been in an operational fuel cell for at least 72 h prior to physical testing) were available. In the case of membrane WO, only an aged sample was available. All other membranes were new membranes. Membranes 522B and 144A were manufactured using exact the same composition, the only difference was the method of catalyst layer dispersion. A film of polypropylene (EXXON PP-7684E2) prepared by melt pressing was used for validation purposes.

2.2. Sample preparation and characterization

Salts used in ion exchange experiments (NaCl , KCl , MgSO_4 , NiCl_2 , and CuSO_4) were purchased from Fisher and BDH Chemicals and were used without additional purification. Salt forms of the membranes were prepared by placing membrane samples in 1 M salt solutions at 80 °C for 24 h,

Table 1
Description of membranes studied

Membrane label	Age	Thickness (mm)	Catalyst	Core membrane	Description
144A	New, used	0.05	Yes	112	Ion Power M37144A
522B	New	0.05	Yes (low dispersion)	112	Ion Power M37522B
WO	Used	0.05	Yes	112	Ion Power WO
555	New	0.05	Yes (high dispersion)	112	Ion Power G37555
112	New	0.04	No		Nafion™
117	New	0.17	No		Nafion™

similar to another method available in the literature [8]. The membranes were stored in the salt solutions until use. The degree of ion exchange was determined by titrating the protons released from the membranes using a 0.1 M NaOH solution [15] with phenolphthalein as an indicator. Since determination of the end-point is based on color change, ion exchange in colored salt solutions (CuSO_4 , NiCl_2) were not tested. Water uptake was determined by taking the dry and wet weights of the samples. The wet weights were taken after the samples had been allowed to hydrate in water for 24 h at 80 °C and the surfaces were blotted dry with filter paper. Some of the membranes were used in a fuel cell and the performance was compared. The fuel cell was operated at Ion Power Inc. at 90 °C and 7 psig, on pure hydrogen and air.

2.3. Mechanical testing

A *Rheometrics* DMTA V dynamic mechanical thermal analyzer was used for determination of stress–strain curves and temperature sweeps of the storage modulus, loss modulus, and mechanical damping. The DMTA was operated in both upright (nominal) position and inverted position. The inverted position was used for hydrated experiments. Hydrated samples were run by placing a beaker of solution underneath the DMTA and submerging the fixture and sample. In the nominal position, temperature control was achieved with the DMTA oven and temperature control software. For hydrated experiments the temperature was monitored using an external temperature probe located approximately 2 mm away from sample. The temperature of water or solution in the beaker was externally controlled within 2 °C of the set point and recorded using a LabView program. The maximum strain was limited to values ranging 1.5–2.4%.

Experiments were done using a rectangular tension fixture with a gap width of 10 mm for dry samples and 5 mm for hydrated samples. The samples were cut from larger sheets to a width of 0.6 cm. Widths and thicknesses were measured using a digital caliper. Stress–strain curves were generated using a strain rate of 0.005 mm/min and an initial static force of 0.1 N at 80 °C. Dynamic experiments also used a frequency of 1 Hz and 0.1 N initial static force. The temperature ramp rate was 2 °C/min at a constant strain of 0.05%. Dry samples were tested from 40 to 140 °C and hydrated samples were tested from ambient temperature to the solution boiling point (approximately 100 °C). Ion exchanged hydrated experiments were conducted with membranes submerged in 1 M solutions of the corresponding salts.

2.4. Validation

Since the DMTA was used in different orientations and with the fixtures immersed in water solutions, validation experiments were conducted to ensure consistency. A polypropylene (PP) film was tested at room temperature in the dry-nominal, dry-inverted, and hydrated-inverted positions. It was assumed that the mechanical properties of PP would not be significantly impacted by submersion in water over short periods of time

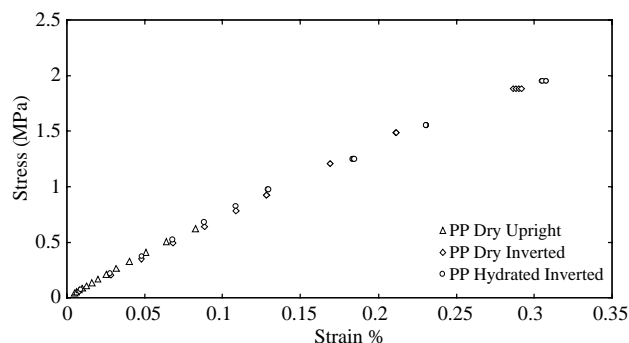


Fig. 2. Stress–strain curves of polypropylene under three different conditions (upright-dry, inverted-dry, and inverted-hydrated, at ambient temperatures).

(<30 min). All three test situations offered the same results (see Fig. 2) indicating that the instrument software was able to compensate for each experimental situation. Hence differences seen on tested membranes were due to changes in their structures consequently to hydration or ion exchange.

Repeatability experiments were also performed to validate the procedure. Due to sample limitations only membrane 522B was used for this phase of the research. Since the materials and fabrication procedures of the catalyzed membranes are similar, the measurement variability of membrane 522B can be applied to the other catalyzed membranes. Measurements of Young's modulus and yield strength produced standard deviation estimates of 0.19%/MPa and 0.14 MPa, respectively. Repetition of temperature sweeps yielded the standard deviation of the transition temperature to be 2.25 °C.

3. Results and discussion

3.1. Ion exchange and hydration

The degree of ion exchange was determined for membrane 112 to confirm that different ions would be taken up by the membrane in comparable amounts. Since all of the catalyzed membrane samples used membrane 112 laminated between the catalyst layers, it was assumed that those catalyzed membranes using membrane 112 as a core electrolyte would have similar ion exchange. Results presented in Table 2 show that the number of moles of ion exchanged by the membrane was similar despite the type of ion. The degree of hydration was also measured for different membranes. Results in Table 3 show similar hydration behavior, except for membrane 117 which showed inferior hydration.

Table 2
Degree of ion exchange in membrane 112 using Na^+ , K^+ , and Mg^{2+}

Ion	Volume of titrant (mL)	Mass of membrane (g)	Specific exchange ($\text{mmol H}^+/\text{g}$)	Degree of ion exchange (mmol ion/g)
H_3O^+	0.2	0.0556	0.09	
Na^+	0.8	0.0762	0.53	0.53
K^+	0.7	0.0550	0.63	0.63
Mg^{2+}	1.2	0.0556	1.07	0.54

Table 3
Degree of hydration (wt%) due to water uptake in membranes

Membrane	Hydration (wt%)
522B	32.1
555	38.6
112	39.2
117	25.6

3.2. Mechanical testing of dry and hydrated membranes

Membrane 117 has thickness of 0.17 mm and has been investigated in several previous studies. The need to minimize the amount of material and the resistance across the MEAs has led to the development of considerable thinner membranes resulting in membrane 112 with thickness of 0.04 mm. This much thinner membrane faces challenges associated with its mechanical properties, specifically integrity failures and pinhole formation in the membranes leads to fuel cell failure. Therefore, for a durable fuel cell, a robust membrane with high mechanical strength, under fuel cell operating conditions, is desired. Fig. 3 shows the stress–strain curves generated for five dry membranes at 80 °C. Table 4 shows the Young's modulus and yield strength data calculated from those plots. Young's modulus is used as an indication of stiffness and yield strength (stress at the intersection of the stress–strain curve with a 0.2% offset) as an indication of the onset of plastic deformation, and therefore, strength.

The differences seen amongst the membranes show that manufacturing and age of membranes had an impact on the material properties. Comparison of the new and aged samples of membrane 144A shows that the Young's modulus and the yield strength have both decreased in the aged sample over the new samples. In general new membranes figured in the upper range with better mechanical modulus and aged membranes (144A aged and W–O) figured in the lower range with inferior modulus. As shown in Fig. 4 yield strength generally increased with increasing Young's modulus.

Mechanical properties in ionomers are attributed to differences in the morphology of backbone, ionic domains, or contributions from both. According to Eisenberg and Kim [16] at temperatures below the glass transition of the ionic domains the clusters would behave as fillers. They are expected to increase the Young's modulus with size. The size of a cluster is

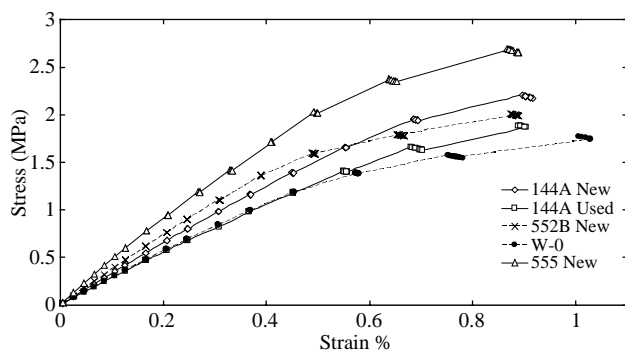


Fig. 3. Stress–strain curves of five catalyzed dry membranes at 80 °C.

Table 4
Young's modulus and yield strength values of dry membranes obtained from stress–strain curves at 80 °C

Membrane	Young's modulus (MPa/%)	Yield strength (MPa)
144A new	3.23	2.19
144A used	2.71	1.88
555 new	4.37	2.5
522B new	3.47	1.82
WO used	2.78	1.55

a function of the equivalent weight of the material. For the case described here all membranes had the same equivalent weight, hence the cluster sizes were expected to be similar, although the manufacturing conditions may impose variability of cluster size in the material. It is not likely that the variation in modulus was due solely to variations in the ionic domain, as will be corroborated with the dynamic mechanical results. Therefore, it is reasonable to assume that the difference in mechanical properties came from the differences in semicrystalline domains (fluorinated hydrophobic backbone) as well as the ionic domain. The membranes with higher Young's modulus and yield strength might have morphology in the semicrystalline domains causing the increase in mechanical stiffness and strength. A possible reason for these differences is through variability in manufacturing process or materials degradation during cell operation (i.e. material aging). Process steps that may impact membrane morphology and consequently mechanical strength include the amount of solvent used in the solution for the casting process and the casting temperature. The process variables associated with the hot pressing of the catalyst layer on to the membrane might have also impacted morphology, i.e. the distribution of crystalline, amorphous and ionic phases in the material.

From an operational standpoint, hydration of the membrane will have a large impact on mechanical properties because water has a plasticization effect on Nafion™ membranes [10]. Fig. 5 shows the difference between membrane 522B under dry and hydrated conditions at 80 °C. On average, the Young's modulus changed by a factor of almost five from 3.47 to 0.73 MPa/%, and the yield strength decreased from 1.82 to 0.86 MPa. These results are similar to those published by Kawano et al. [8] who reported a decrease in Young's modulus

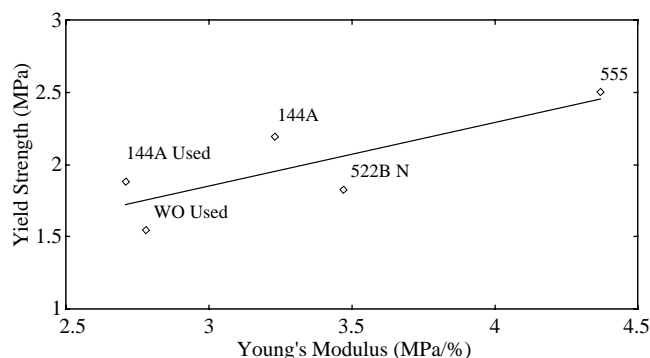


Fig. 4. Plot of Young's modulus versus yield strength for five catalyzed membranes.

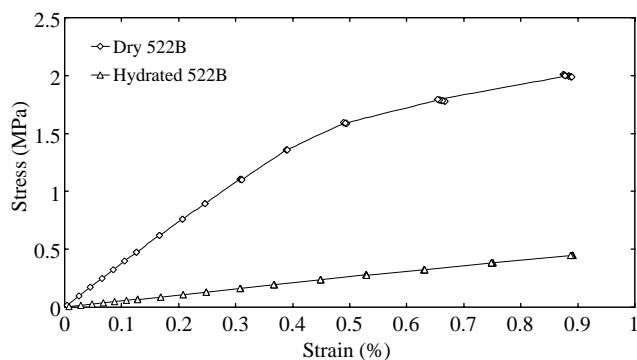


Fig. 5. Comparison of stress/strain curve for the 522B MEA under hydrated and dry conditions at 80 °C.

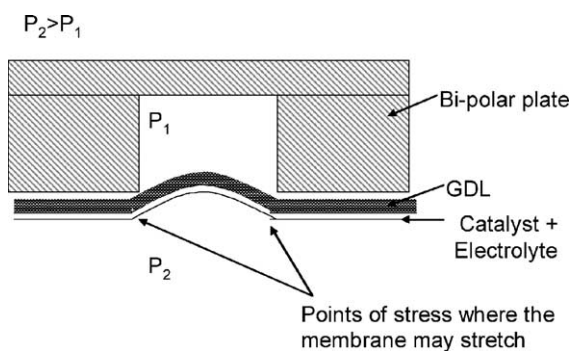


Fig. 6. Schematic of the stress on a pinched MEA in a PEMFC.

from 2 to 0.95 MPa/% at 27 °C (note that the method of hydration was different). The hydrated results are also similar to the Young's modulus of approximately 0.34 MPa/% obtained using a similar method of hydration at 80 °C produced by Budinski and coworkers [17].

Hydration of membranes has a significant effect on the polymer: (a) the membrane swells as the ionic regions grow with the addition of more water; and (b) the side chains with ionic end groups become more mobile. This latter effect has a major implication on ionic conduction in the membrane. The increased mobility allows hydrogen to be passed from one sulphonic acid group to another. Unfortunately, these two

effects also act to decrease the stiffness and the yield strength. In particular, as the ionic channels swell the separation between ionic chain termination increases causing a decrease in the intermolecular forces within ionic clusters.

The main implication of reduced Young's modulus and yield strength is that it makes the membrane susceptible to permanent deformation, gradual weakening, and eventual failure in a fuel cell when exposed to pressure gradients and pressure pulses. This important aspect is highlighted through the practical need for thinner membranes without compromising durability. Fig. 6 illustrates the stress points created on the membrane inside the fuel cell by the pinching action of the bi-polar plate lands (which distribute reactants) on the membrane when a pressure differential exists across the membrane. Fig. 7 shows an extreme example of the type of failure that can be caused by this situation. The failure in Fig. 7A was caused by a large pressure differential in the fuel cell and a channel width that was too wide to mechanically support the membrane (Fig. 7B).

Attempts at Ion Power Inc. to improve mechanical properties of MEAs and to reduce the amount of Nafion™, and consequently the material and manufacturing costs, have involved using a polyimide film (Kapton™) as a membrane frame in order to increase the strength on the edge of the active area of the MEA. Studies of mechanical properties of these materials under hydrated conditions have shown an improvement on yield strength of membranes framed in polyimide films. Budinski and coworkers have found that the MEA/polyimide interface had a higher load-carrying capacity than the MEA active area [17].

3.3. Mechanical testing of membranes after ion exchange

Samples of membranes 522B, 555, 112, and 117 were exchanged with different ions and were tested while submerged in salt solutions. The ions included both monovalent and divalent types with a range of ionic radii. Fig. 8 compares the Young's modulus of four hydrated membranes before and after ion exchange. Before ion exchange the hydrated membranes are in the acid form and contain H_3O^+ . For comparison, the H_3O^+ radius was approximated as the atomic radius of an oxygen

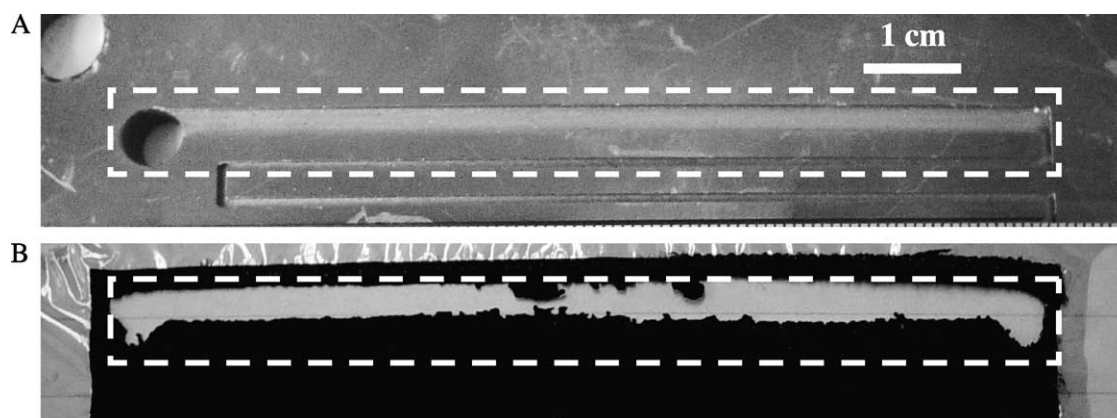


Fig. 7. Photograph of a failed MEA as result of differential pressure across the MEA. Bipolar plate with an extra wide channel (top) which participated in the formation of a tear in the MEA (bottom).

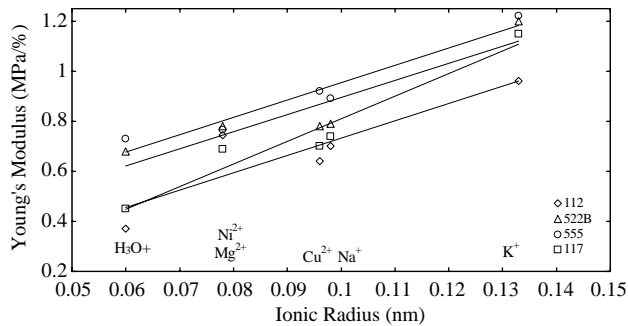


Fig. 8. Impact of ionic radius on the Young's modulus of catalyzed and uncatalyzed membranes. The lines illustrate the increasing trends.

atom. The results show that with increasing radius the Young's modulus increased. Similar results were also achieved with the yield strength as shown in Fig. 9. All of the hydrated and exchanged samples had Young's moduli and yield strengths that were smaller than their dry counterparts. These results follow the same trend as those reported by Kawano et al. [8] on dried membranes exchanged with monovalent alkali metals.

The increase of Young's modulus and yield strength is largely attributed to a physical crosslinking effect that occurs in the ionic clusters. The addition of ions increased the ionic interactions in the clusters, therefore, reducing chain mobility and increasing stiffness and strength. Interestingly, the charge on the salt had no perceptible impact on the results. It was originally expected that the Young's modulus and yield strength would be larger with the addition of divalent ions than with the addition of monovalent ions because of the higher charge density. One would expect that divalent atoms could make two ionic bonds with the sulphonic acid groups further increasing the crosslinking effect, i.e. in order to maintain a charge balance, twice the number of sulphonic acid groups would become associated with the divalent ions than the monovalent ones. This was observed in the titrations results done after ion exchange where, for the same molar amount of ions incorporated into the membrane, there was twice the number of hydrogen ions released for the divalent ion tested. However, the ionic radius seemed to be the single largest factor governing the impact on the mechanical properties. This is attributed to the surface area available to the ionic side chains as the limiting factor for the physical crosslinking. Although the divalent ions may have a higher charge density, they might

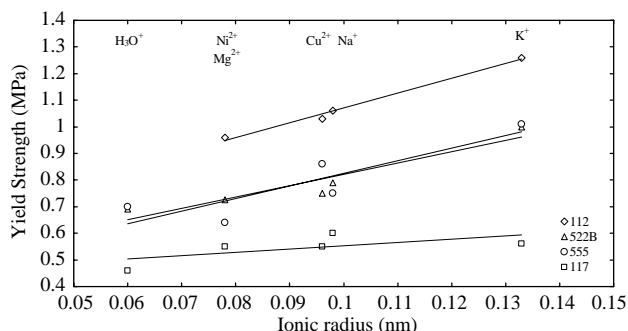


Fig. 9. Impact of ionic radius on the yield strength of catalyzed and uncatalyzed membranes. The lines illustrate the increasing trends.

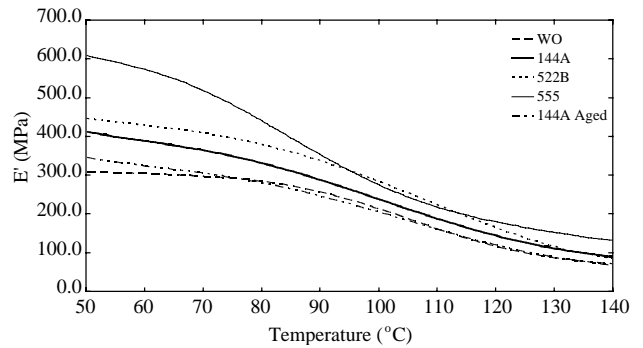


Fig. 10. Change of storage modulus with temperature of five catalyzed membranes.

not have enough surface area available for side chains to take advantage of it.

From the graph of Young's modulus the catalyzed membranes were typically stiffer than the uncatalyzed membranes. This was an expected result since the catalyst layer coating is not as flexible as a pure Nafion™ membrane. This trend is not followed by the yield strength results. It is not entirely clear why membrane 112 would have larger yield strengths over the catalyzed membranes. Recall that the catalyzed membranes were two catalyst layers that are laminated to the two sides of a Nafion™ 112 membrane. It is possible that the extra processing steps used to add catalyst to the membrane has increase the number of defects on interface Nafion™/catalyst layer and consequently reduced the yield strength. Note that the hydrated samples that did not use ion exchange showed the expected trend.

There are several implications of these results. Apart from the damaging effect that contaminant ions have on the ability of the membrane to conduct protons, they also change the mechanical properties of the membrane. The increase in the Young's modulus means that the material becomes stiffer, a larger force is necessary to cause elastic deformation. The increased yield strength may serve to keep the membrane from plastic deformation when strained.

3.4. Dynamic mechanical testing of dry membranes

In order to examine temperature transitions the membranes underwent dynamic mechanical thermal testing. Figs. 10 and 11 shows plots of E' (storage modulus) and E'' (loss modulus)

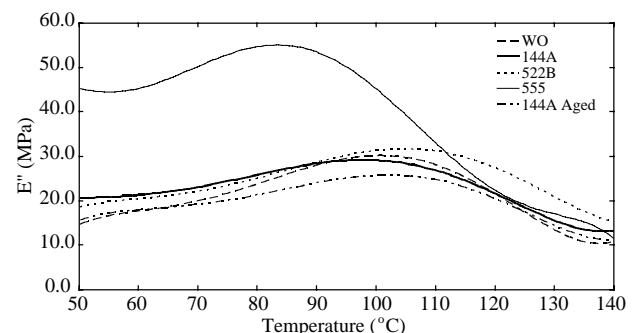


Fig. 11. Change of loss modulus with temperature of five catalyzed membranes.

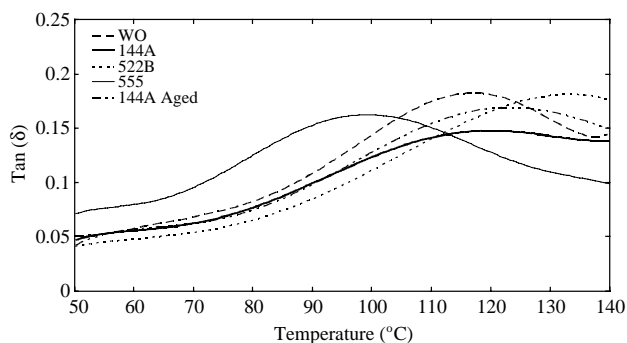


Fig. 12. Change of $\tan(\delta)$ with temperature of five catalyzed membranes.

versus temperature, respectively; Fig. 12 shows $\tan(\delta)$ (mechanical damping) versus temperature for each of the membranes; and Table 5 identifies the transition temperature for dry membranes. The upper glass transition temperature (α -transition) represents the temperature where the ionic clusters become mobile in Nafion™.

It is important to understand the behavior of membranes in the vicinity of 80 °C because this is the temperature of operation in many fuel cell applications. Curves in Fig. 10 show a change in storage modulus over a large temperature range. Above 80 °C there was a continuous loss in stiffness as shown by the drop in E' of dry membranes. The loss modulus (Fig. 11) showed a transition happening between 70 and 140 °C, representing change in elastic behavior of these membranes. Unlike the Young's modulus values, the transition temperature between new and aged membrane 144A did not change significantly. Also, there was no trend when comparing the aged membranes (membrane 144A and WO) to the new membranes.

It is possible that the mobility of ionic clusters measured by mechanical damping can be related to fuel cell performance. Results obtained for dry membranes (Fig. 12) showed there were significant differences of the transition temperatures between membranes 522B and 144A. The α -transition temperature was lower for membrane 144A. Membranes 144A and 522B were tested in a fuel cell and the polarization curves are shown in Fig. 13. Membrane 144A had less ohmic losses than membrane 522B. Though the results are not conclusive, they could be attributed to a higher mobility of ionic domains in membrane 144A than in membrane 522B and consequently higher mobility of protons during fuel cell operation at a temperature of 90 °C.

Table 5
Glass transition temperature (α -transition) for dry membranes obtained from mechanical damping measurements

Membrane	Glass transition temperature (°C)
144A (new)	121
144A (used)	124
555 (new)	99
522B (new)	135.2
WO (used)	116

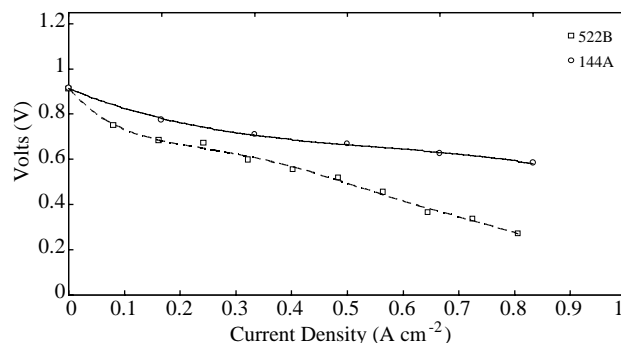


Fig. 13. Comparison of fuel cell performance of membrane 522B and membrane 144A.

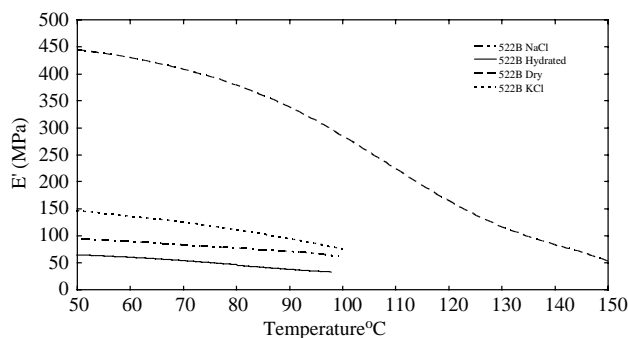


Fig. 14. Comparison of storage moduli of membrane 522B in dry, hydrated, and exchanged with KCl and NaCl.

3.5. Dynamic mechanical testing of hydrated membranes

Operating the fuel cell at temperatures closer to the α -transition would have benefits to performance since the ionic domains of the membrane will be more mobile and hence be able to transport protons with less resistance. Figs. 14–16 show the E' , E'' , and $\tan(\delta)$ curves for membrane 522B in dry, hydrated, and exchanged (Na^+ and K^+) forms. Temperature sweeps of the hydrated membranes showed that E' and E'' were higher in the dry samples than in the hydrated samples. Table 6 shows the E' of membrane 522B dropped from almost a full order of magnitude at 80 and 50 °C between the dry membrane and the water saturated membrane, following the same trend observed for Young's modulus results. The E'' results

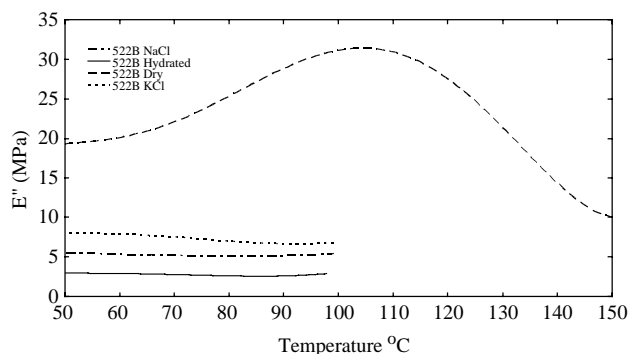


Fig. 15. Comparison of loss moduli of membrane 522B in dry, hydrated, and exchanged with KCl and NaCl.

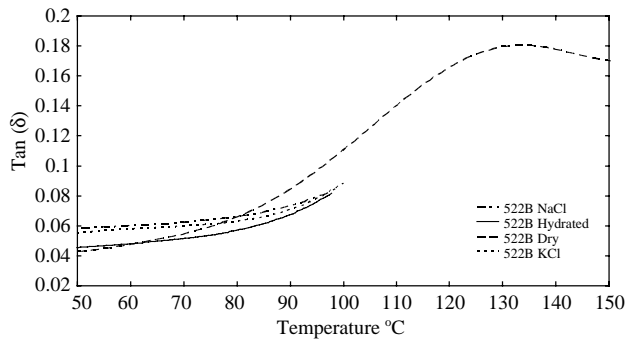


Fig. 16. Comparison of $\tan(\delta)$ of membrane 522B in dry, hydrated, and exchanged with KCl and NaCl.

demonstrated a similar decrease in magnitude. It was also observed that increasing ionic radius of the contaminant ion increased the values of E' and E'' . The addition of Na^+ ion increased the value of E' and E'' at both 50 and 80 °C by 50%. With the addition of KCl the increase was over 100%.

The storage modulus of both the dry and hydrated case showed an overall decreasing trend over the temperature range, however, the rate of change was larger for the dry case. The hydrated curves did not show a dramatic change over the temperature range as the dry sample. The E' measurements of the hydrated sample at 100 °C are on the same order as the E' measurements of the dry sample after the dry transition temperature of 135 °C indicating that hydration imparts as much mobility on the ionic domain as temperature does with the dry membrane. With the loss modulus results, the curve for the dry membrane rose and reached a peak near 100 °C before dropping. In the hydrated cases there is little change in the loss modulus.

The curves of $\tan(\delta)$ showed different trends compared to the graphs of storage and loss modulus. In all cases the curves of the hydrated and salt cases started at higher $\tan(\delta)$ values than the dry case. However, they eventually crossed under the $\tan(\delta)$ curve of the dry membrane. In the experimental temperature range, the values of the mechanical damping remained similar between the dry and the hydrated membrane. The α -transition temperatures of the hydrated samples could not be measured because the transitions did not appear at temperatures lower than 100 °C. Therefore, the onset temperatures of the α -transition were compared. Fig. 17 and Table 6

Table 6
Storage and loss moduli at 50 and 80 °C and onset of α -transition temperature for dry, hydrated and ion exchanged membrane 522B

	Temperature (°C)	Dry	Hydrated	Na^+	K^+
E' (MPa)	50	444	64	96	144
E'' (MPa)	50	19	2.8	5.6	7.9
E' (MPa)	80	378	49	78	113
E'' (MPa)	80	25	2.8	5.2	7.3
Onset α -transition (°C)		78	67	79	86

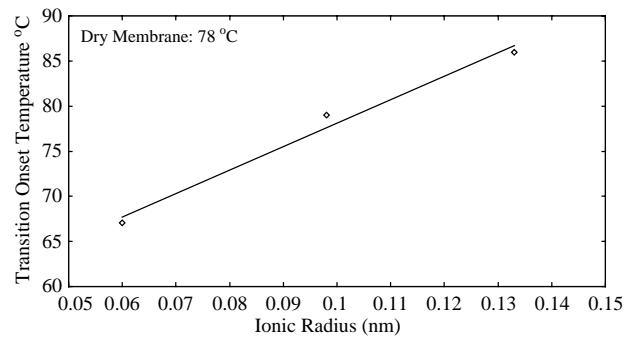


Fig. 17. Relationship between transition onset temperature and ionic radius of exchanged salts. The line illustrates the increasing trend.

illustrate the impact of ionic radius of contaminant ions on the onset temperature of α -transition.

The results show that ion exchange increased the onset temperature of the α -transition and the values of E' and E'' on hydrated membranes. This follows the same interpretation used for the dry membranes, that ions increase physical crosslinking (due electrostatic attraction between ions of opposite charges) in the ionic domains. In the dry state, the ionic domain was less mobile and in the case of membrane 522B the onset temperature for α -transition was 86 °C. Hydration led the ionic regions to absorb water and swell to consequently increase mobility in the ionic domain. As a consequence of improved mobility on the set temperature for the α -transition decreased to 67 °C. This result has shown that although hydration decreases the transition onset temperature, the actual transition temperature remains outside the normal operating range of a fuel cell. Ion exchange decreased mobility in the ionic domains: addition of Na^+ brought the onset temperature of α -transition to a value slightly higher than the dry case; addition of K^+ increased the onset temperature 8 °C above the dry case.

4. Conclusions

Mechanical properties of Nafion™ 112 membranes (thinner) and Nafion™ 117 and catalyzed membranes made using Nafion™ 112 as core electrolyte were measured in dry and hydrated conditions. Ion exchange has shown to dramatically affect mechanical properties of membranes under hydrated conditions.

There was significant variation in Young's modulus, ranging 4.37–2.71 MPa/%, and yield strength, ranging 1.82–2.50 MPa, among different catalyzed membranes. This was attributed to manufacturing conditions that could have impacted morphological distribution on the membranes (crystallinity of the hydrophobic domain and possibly the ionic cluster size). The Young's modulus and yield strength decreased with hydration by almost an order of magnitude, from 3.47 to 0.73 MPa/%, due to the plasticization effect of water. Ion exchange in hydrated membranes increased stiffness compared to the hydrated membranes without ion exchange. This was attributed to the physical crosslinking on the ionic domains of the membranes whereby salt ions provided sites

where the sulfonic acid groups could link. The Young's modulus and the yield strength were found to increase with increasing ionic radius.

Dynamic mechanical measurements of transition temperature showed variations between different membranes due to manufacturing differences. Hydration has decreased both the storage and loss moduli and the onset temperature of α -transition. Lower α -transition temperatures might correspond to better proton mobility during fuel cell operation; however, more studies are needed in this area. With the addition of Na^+ and K^+ the onset temperature of α -transition increased when compared to the hydrated form with increasing ionic radius. Decreases in membrane stiffness and strength that occur in the membrane as a result of hydration and ion exchange could impact the performance and structural stability in a fuel cell which in turn would result in overall durability of the fuel cell.

Acknowledgements

The authors would like to acknowledge Ion Power Inc. for supporting this study; Michael Budinski at General Motors for sharing information used as reference; and the Natural Sciences and Engineering Research Council (NSERC) of Canada for financial support.

References

- [1] Fowler MW, Mann RF, Amphlett JC, Peppley BA, Roberge PR. *J Power Sources* 2002;106(2):274–83.
- [2] Lehmani A, Durand-Vidal S, Turq P. *J Appl Polym Sci* 1998;68(3):503–8.
- [3] Xue T, Trent JS, Osseo-asare K. *J Membr Sci* 2000;45:261–71.
- [4] Haubold H, Vad T, Jungbluth H, Hiller P. *Electrochim Acta* 2001;46(10):1559–63.
- [5] Okada T. *J Electroanal Chem* 1999;465(1):1–17.
- [6] Pozio A, Silva RF, De Francesco M, Giorgi L. *Electrochim Acta* 2003;48(11):1543–9.
- [7] Liu W, Ruth K, Rusch G. *J New Mater Electrochem Sys* 2001;4:227–31.
- [8] Kawano Y, Wang Y, Palmer RA, Aubuchon SR. *Polim Cien Tecnol* 2002;12:96–101.
- [9] Yeo SC, Eisenberg A. *J Appl Polym Sci* 1977;21:875–98.
- [10] Uan-Zo-Li JT. The effects of structure, humidity and aging on the mechanical properties of polymeric ionomers for fuel cell applications. MSc Thesis. Virginia Polytechnic Institute and State University, Blacksburg, VA, USA; 2001.
- [11] Almeida SH, Kawano Y. *J Ther Anal Calor* 1999;58:569–77.
- [12] Stefanithis ID, Mauritz KA. *Macromolecules* 1990;23:2397–402.
- [13] Laporta M, Pegoraro M, Zanderighi L. *Macromol Mater Eng* 2000;282:22–9.
- [14] Kyu T, Eisenberg A. *J Polym Sci Polym Symp* 1984;71:203–19.
- [15] Scherer R, Bernardes AM, Forte MMC, Ferreira JZ, Ferreira CA. *Mater Chem Phys* 2001;71:131–6.
- [16] Eisenberg A, Kim J. *Introduction to ionomers*. New York: Wiley; 1998.
- [17] Budinski M, Cook A, Atkins D. Private communication. General Motors; 2004.